Case Studies in Chemical and Environmental Engineering 10 (2024) 100781

Contents lists available at ScienceDirect

Case Studies in Chemical and Environmental Engineering

journal homepage: www.sciencedirect.com/journal/case-studies-in-chemical-and-environmental-engineering

Case Report

Calcination-modified zeolite filtration and UV disinfection for contaminant Mitigation in groundwater

Kulyash Meiramkulova [a], Aliya Kydyrbekova [a,*], Timoth Mkilima [b], Tursynkul Bazarbayeva [c], Umbetova Sholpan [d], Mansur Zarbaliyev [e], Tatyana Uryumtseva [f], Laura Kurbanova [c], Bayan Tussupova [c], Mikhail Zhumagulov [g]

[a] Research Institute of Environment and Water Management, L.N. Gumilyov Eurasian National University, Satpayev Street 2, 010000, Astana, Kazakhstan
[b] Department of Environmental Engineering and Management, The University of Dodoma, Dodoma, P.O. Box 259, Tanzania
[c] Department of the UNESCO Chair for Sustainable Development, Al–Farabi Kazakh National University, Al–Farabi 71, 050040, Almaty, Kazakhstan
[d] Department Water and Land Management, Korkyt Ata Kyzylorda University, Aiteke Bi street 29 A, 120014, Kyzylorda, Kazakhstan
[e] Department "Reclamation and Water Management Construction "Azerbaijan University of Architecture and Construction, Baku A.Sultanova Street 11, AZ, 1073, Azerbaijan
[f] Department of Veterinary Medicine and Industrial Technologies, LLP Innovative University of Eurasia, Lomov str.45, 140000, Pavlodar, Kazakhstan
[g] Department of Thermal Engineering, L.N. Gumilyov Eurasian National University, Satpayev Street 2, Astana 010000, Kazakhstan

ARTICLE INFO

Keywords:
Water treatment
Sustainability
Zeolite modification
Ultraviolet treatment
Contaminant removal
Groundwater quality

ABSTRACT

Access to safe drinking water is a pressing global concern, necessitating innovative purification methods. This study investigated the efficacy of combining calcination-modified zeolite filtration with ultraviolet (UV) disinfection to mitigate microbial contamination in raw groundwater. A comparison was made between the treatment system employing calcination-modified natural zeolite and the system utilizing natural zeolite without modification. Results from isotherm and kinetic modeling revealed enhanced adsorption behavior and mechanisms in modified zeolite compared to its natural counterpart, leading to improved adsorption capacity and kinetics. Enhancements in removal efficiencies were observed for contaminants such as zinc, cadmium, and manganese, with increases from 30.25 % to 67.5 %, 55.75 %–82.75 %, and 64.04 %–69.52 %, respectively. Similarly, enhanced removal efficiencies for organic contaminants like phenol and cyanides were noted, rising from 59.99 % to 73.26 % and 59.22 %–65.05 %, respectively, with the modified zeolite. Furthermore, filtration with both natural and modified zeolites coupled with UV disinfection substantially reduced microbial contamination levels in raw groundwater, with total coliforms decreasing from 2245 CFU/mL to 8 CFU/mL post-filtration and UV treatment. Notably, surface area increased from 60 m^2/g to 220 m^2/g, and pore volume increased from 0.15 cm^3/g to 0.8 cm^3/g for modified zeolite. These findings underscore the potent antimicrobial efficacy and improved adsorption performance of the combined approach, contributing to advancing water purification technologies and addressing critical global health challenges.

1. Introduction

Groundwater, essential for human consumption and supporting diverse industrial activities, remains vulnerable to contamination from various sources. Contaminants such as heavy metals, organic compounds, and microbial pathogens pose significant risks to its usability, threatening public health and environmental sustainability [1,2]. The urgency to safeguard this vital resource underscores the critical need for effective purification methods. Groundwater contamination can stem from both natural and anthropogenic sources, including agricultural runoff, industrial discharge, and improper waste disposal [3]. Pesticides and fertilizers used in farming can leach into groundwater, introducing harmful chemicals like nitrates and phosphates [4]. Similarly, industrial activities release heavy metals such as lead, mercury, and arsenic into the ground, endangering both groundwater quality and the ecosystems it supports [5]. Moreover, improper sewage disposal or malfunctioning

* Corresponding author.
E-mail addresses: kuleke@gmail.com (K. Meiramkulova), aliyafromkz@gmail.com (A. Kydyrbekova), tmkilima@gmail.com (T. Mkilima), tursynkul.bazarbayeva@gmail.com (T. Bazarbayeva), umbetova-37@mail.ru (U. Sholpan), zarbaliyev.m@mail.ru (M. Zarbaliyev), vbh2@mail.ru (T. Uryumtseva), Kurbanova.Laura@kaznu.kz (L. Kurbanova), tussupova@yandex.ru (B. Tussupova).

https://doi.org/10.1016/j.cscee.2024.100781
Received 26 April 2024; Received in revised form 25 May 2024; Accepted 28 May 2024
Available online 30 May 2024

septic systems can introduce microbial pathogens like *E. coli* and *Giardia* into groundwater, posing severe health risks to nearby communities [6].

Furthermore, the effectiveness of groundwater purification technologies can be influenced by various factors, including the specific contaminants present, geological characteristics of the aquifer, and local regulatory standards. For instance, while membrane filtration [7], offers high removal efficiency for contaminants like bacteria and viruses, it may be less effective against certain organic compounds or heavy metals. Similarly, electrochemical remediation techniques [8], show promise for treating metal contaminants but may require significant energy inputs and maintenance costs. Moreover, in remote or underserved areas, logistical challenges such as transportation of equipment and skilled personnel can hinder the implementation of advanced purification methods. Consequently, achieving widespread access to clean groundwater necessitates not only technological innovation but also holistic approaches that address socioeconomic disparities and institutional capacity-building. The quest for equilibrium between cost and efficiency in groundwater purification is not only a global concern but also a pressing environmental issue that demands immediate attention [9]. The impact of groundwater contamination extends beyond geographical boundaries, affecting both developed and developing regions and exacerbating socioeconomic disparities. Communities with limited resources are particularly burdened, as they must navigate the complex trade-offs between investing in advanced purification technologies and fulfilling their immediate water needs [10]. Furthermore, as societies strive to ensure equitable access to clean and safe water resources, it is imperative to explore and implement innovative purification strategies that are both effective and economically viable [11]. Through interdisciplinary research and collaborative efforts, the communities can advance toward sustainable solutions that protect groundwater quality, mitigate environmental risks, and promote public well-being [12].

Conventional methods for groundwater treatment often face limitations that can hinder their effectiveness in fully addressing the diverse array of contaminants present in groundwater. These methods, such as filtration [13], coagulation [14], and chlorination [15], may struggle to efficiently remove certain pollutants, especially those of a chemical or microbial nature, due to their inherent constraints. For instance, filtration methods may be inadequate for the removal of dissolved organic compounds or pathogens, while chlorination can produce harmful disinfection by-products. Additionally, some conventional treatment approaches require extensive infrastructure and resources, making them economically and logistically challenging, particularly in rural or resource-limited settings. The integration of calcination-modified zeolite and Ultraviolet Light-Emitting Diode (UV-LED) disinfection presents a promising alternative by capitalizing on the unique properties of both technologies. Calcination modification enhances the adsorption capacity of zeolite for a wide range of contaminants, while UV-LED disinfection provides a chemical-free and energy-efficient method for microbial inactivation.

Natural zeolite is a porous material with excellent adsorption capabilities, capable of selectively removing a wide range of contaminants from water [16–18]. UV LED technology, on the other hand, offers a highly efficient and environmentally friendly method for disinfection, effectively eliminating pathogens and reducing the risk of waterborne diseases [19]. Natural zeolite is formed when volcanic ash and groundwater interact over long periods, resulting in a crystalline structure with a high surface area and unique adsorption properties. In water purification, natural zeolite acts as a filtration medium [20]. Its porous structure allows it to trap and adsorb various contaminants present in water, including heavy metals, ammonium, organic compounds, and certain radioactive substances [21]. The adsorption process occurs when the contaminants come into contact with the zeolite's surface, where they are attracted and held in the pores. The adsorption capacity of natural zeolite is attributed to its ion-exchange properties. The zeolite framework contains channels and cavities that can accommodate ions of different sizes and charges. As water passes through these channels, the zeolite selectively captures and exchanges ions, removing harmful substances from the water [22]. However, to improve its effectiveness in water treatment, natural zeolite is modified to enhance its adsorption capacity and selectivity, enabling more efficient removal of contaminants from water sources. Various approaches for enhancing natural zeolite have been documented in the literature. For instance, Kuldeyev et al. [23], explored the impact of thermal activation on the adsorption capacity of natural zeolite. Their findings revealed that thermal activation, achieved through furnace treatment, significantly augmented the zeolite's adsorption capacity for heavy metals. Other techniques encompass methods such as the utilization of lanthanum and hexadecyl trimethyl ammonium bromide [24], acid and alkaline treatment [25], as well as functionalization and hydrothermal treatment [26]. Despite these various efforts, there is still a lack of information regarding the modification of natural zeolite through calcination for the treatment of groundwater.

Moreover, in the literature, various studies have explored the potential of zeolite-based treatments for water. For instance, Li et al. [27], conducted research on ammonium removal from groundwater utilizing a zeolite permeable reactive barrier, as demonstrated in a pilot-scale study. The findings revealed that under lower redox conditions, denitrifying bacteria inhabiting the zeolite facilitated the removal of nitrate formed during nitrification. Throughout the extended operational period lasting 328 days, more than 90 % of $NH4^{+}$-N was consistently eliminated, with approximately 40 % of the influent $NH4^{+}$-N being oxidized to nitrate. Subsequently, after 300 days of operation, up to 60 % of the nitrate generated within the permeable reactive barrier was reduced within the zeolite layer. Siemens et al. [28], investigated sodium adsorption using reusable zeolite adsorbents, while Kwakye-Awuah et al. [29], explored the adsorptive removal of iron and manganese from groundwater. Additionally, Yogafanny et al. [30], studied the treatment of brackish groundwater. However, despite endeavors to investigate the capabilities of natural and modified zeolite for water treatment, there remains a scarcity of information regarding the potential of calcination-modified zeolite for groundwater treatment, let alone the potential integration of zeolite-based materials and UV disinfection for this purpose.

As previously highlighted, UV-LED technology, on the other hand, is a highly efficient method used for disinfection in water treatment. UV light in the germicidal range (UV–C) possesses the ability to deactivate microorganisms, including bacteria, viruses, and protozoa, by damaging their deoxyribonucleic acid (DNA) or ribonucleic acid (RNA) [31]. UV-LEDs emit UV-C light at specific wavelengths that are lethal to microorganisms while being safe for human exposure [32]. UV-LED disinfection works by exposing the water to UV-C light as it passes through a chamber containing the UV-LED sources. The UV light penetrates the cells of microorganisms, disrupting their genetic material and rendering them unable to reproduce or cause infection. It provides an effective means of disinfection without the use of chemicals, and the process does not introduce any harmful byproducts into the water [33].

This study aims to investigate the integration of natural zeolite and UV LED disinfection for groundwater purification. By examining the synergistic effects of these technologies, the study seeks to assess their efficacy in removing a wide range of contaminants from groundwater sources. Additionally, the research aims to evaluate the economic viability and scalability of this integrated approach, providing valuable insights for future water purification strategies. Through rigorous experimentation and analysis, this study endeavors to contribute to the advancement of sustainable solutions for ensuring access to clean and safe groundwater resources.

2. Materials and methods

2.1. Case study description

The groundwater samples utilized in the study were collected from the Tselinograd District in Kazakhstan, located at approximately latitude 50.9585° N and longitude 70.9230° E. In the Akmola Region, groundwater constitutes about 14 % of the total river runoff, although in notably dry years, this proportion increases significantly. Over several years, the total mineralization of river waters in the area decreases from 1500 mg/L near Kamenny Quarry to 450 mg/L at the river mouth. This heightened mineral content is primarily due to the hydroclimatic conditions of the basin, characterized by a high prevalence of evaporation over precipitation. The moisture coefficient of the basin area, indicating the ratio of precipitation to evaporation, is approximately 0.5, underscoring the natural imbalance between heat and moisture resources. The arid climate of the region leads to the accumulation of mineral salts in soils and across the landscape. The Ishim River and its tributaries receive an increased influx of these salts from melting water runoff within the catchment area [34]. Furthermore, the substantial mineralization of groundwater can be attributed to the arid climate. The hydrochemical composition of the river varies annually and seasonally based on discharge rates, yet a recurring pattern emerges: calcium cations dominate in the southern stream, while hydrocarbonates dominate among the anions. Downstream of Astana, especially during flood periods, a chloride-hydrocarbon composition is observed, with calcium ions prevailing among the anions. Along the Sergeevskoye reservoir and up to the outlet portion near the village of Dolmatovo, the hydrocarbonate class of the calcium or sodium group prevails. Water hardness indicators range from 2.95 to 3.88 mg/eq. during spring floods, 4–5.6 mg/eq. during summer or autumn low-water periods, and 6.0–8.4 mg/eq. during winter. The overall oxygen level of the river has consistently been rated as good, with the lowest oxygen content observed during freeze-up periods. Typically, dissolved oxygen content reaches 88 % saturation [34].

2.2. Groundwater sampling

As previously highlighted, groundwater samples for this study were collected from multiple wells within the Tselinograd District, Kazakhstan, specifically at latitude 50.9585° N and longitude 70.9230° E. Each well was purged prior to sampling to remove stagnant water and ensure a fresh groundwater sample, typically involving the extraction of three well volumes. Sterilized submersible pumps were used to draw water from a consistent depth, ensuring uniform sampling conditions. The groundwater was collected directly into 1-L polyethylene bottles that had been pre-rinsed with the sampled water to minimize contamination. Field measurements, including pH were recorded immediately using portable meters to capture in-situ conditions. Samples were then sealed tightly, labeled with the sampling date, time, and location, and stored in coolers at approximately 4 °C to preserve their chemical integrity during transport to the laboratory. In the laboratory, samples were analyzed for key parameters, including total dissolved solids, major cations, and anions. Quality assurance and quality control (Q_A/Q_C) protocols were strictly followed, including the use of field blanks, duplicates, and calibration standards to ensure data accuracy and reliability.

2.3. Material characterization

Table 1 provides a comprehensive overview of the material properties of natural zeolite, specifically clinoptilolite, used in the investigation. Clinoptilolite, composed of microporous silica and alumina tetrahedra, exhibits varying concentrations of essential elements crucial for its adsorption and purification capabilities. Interestingly, the sodium concentrations in clinoptilolite typically outweigh potassium concentrations, aligning with conventional expectations. However, noteworthy exceptions exist, with some sources boasting high potassium content and low sodium levels, offering unique characteristics for specific applications. The natural zeolite samples (Himiya i Tehnologiya, TOO, Almaty, Kazakhstan) displayed varied compositions, as shown in Table 1 (data provided by the supplier). Notably, they exhibited elevated concentrations of SiO_2 and Al_2O_3, indicative of their robust adsorption potential and suitability for groundwater purification endeavors. Each parameter, ranging from CaO to H_2O, delineates the elemental composition of the natural zeolite samples, offering valuable insights into their chemical makeup. These properties play a pivotal role in determining the efficiency and effectiveness of zeolite-based purification processes, underscoring the significance of material characterization in research and practical applications. In essence, Table 1 serves as a comprehensive reference, encapsulating the diverse material attributes of natural zeolite, crucial for understanding its suitability and performance in groundwater purification initiatives.

Table 1
Material properties of natural zeolite.

Parameter	Concentration (%)
CaO	0.1 to 6.4
MgO	0 to 2.1
MnO_2	0.1 to 0.2
Fe_2O_3	1.4 to 5.8
TiO_2	0.1 to 0.7
Al_2O_3	14.0 to 15.0
SiO_2	60.0 to 74.0
Na_2O	0.6 to 5.5
K_2O	0.7 to 4.0
P_2O_5	0.1 to 0.2
H_2O	0 to 4.1

2.4. Natural zeolite modification

The natural zeolite underwent enhancement solely through the calcination method. The process commenced by placing the zeolite samples in a controlled atmosphere furnace, where they were heated at temperatures ranging between 500 °C and 800 °C for a duration of 2–4 hours. This controlled thermal treatment aimed to induce significant alterations in the zeolite's physicochemical properties by effectively eliminating adsorbed water molecules, organic contaminants, and volatile impurities from its structure. Specifically, the objective was to augment the zeolite's surface area, pore volume, and reactivity through the removal of these impurities. Subsequent to the calcination process, the modified zeolite samples underwent meticulous characterization utilizing Brunauer-Emmett-Teller (BET) analysis.

2.5. Brunauer-Emmett-Teller (BET) analysis

Brunauer-Emmett-Teller (BET) analysis was conducted to quantify the surface area and pore characteristics of the natural zeolite before and after the calcination process. Prior to analysis, the zeolite samples were degassed under vacuum to remove any adsorbed moisture and impurities. Nitrogen gas adsorption-desorption isotherms were then recorded at liquid nitrogen temperature (−196 °C) using a high-resolution surface area analyzer. The BET-specific surface area was calculated from the adsorption isotherm data using the multipoint BET method, while the pore size distribution and total pore volume were determined via the Barrett-Joyner-Halenda (BJH) method based on the desorption branch of the isotherm. This detailed analysis provided precise quantitative data on the changes in surface area, pore volume, and pore size distribution induced by the calcination treatment, allowing for a thorough evaluation of the efficacy of this method in enhancing the zeolite's adsorption capacity.

2.6. Experimental setup

The cleaning system operates in a sequential manner as depicted in Fig. 1. Initially, wastewater enters the initial storage tank (1), with a capacity of 2 L. To maintain a constant pressure within the system, the outlet pipe from the tank (1) is strategically positioned at the bottom to utilize the natural backwater effect (liquid column inlet pressure) for the subsequent pump (2). The pump (2) is responsible for providing the necessary pressure for the filtration system, typically ranging from 2 to 4 bar. The first stage of water treatment involves passing the contaminated water through a Zeolite Filter (3). The core of this filter is packed with finely crushed zeolite, which effectively targets and removes hardness salts present in the water. Subsequently, the water undergoes the second stage of cleaning in the UV Treatment Tank (4). Here, it is exposed to ultraviolet radiation emitted by a UV lamp (5), which consists of an array of UV LED lamps. These lamps emit UV light at wavelengths comparable to traditional UV lamps but offer significant advantages in power consumption, contributing to overall energy efficiency. Following UV treatment, the water proceeds to the third step, which involves passage through a Fine Filter (6). This filter serves to further purify the water by capturing any residual biological matter that may have formed during the UV treatment process, ensuring the final product meets stringent quality standards. In parallel, UV LED disinfection experiments were conducted using a custom-designed UV reactor equipped with UV LED lamps emitting at a wavelength of 265 nm, optimized for microbial inactivation. The reactor had a volume of 500 mL and was operated at a flow rate of 100 mL/min to ensure continuous circulation of the groundwater samples. The UV dose was varied from 10 mJ/cm^2 to 50 mJ/cm^2 by adjusting the exposure time accordingly. The samples were continuously circulated through the UV reactor, and aliquots were withdrawn at 5-min intervals for up to 30 minutes. The reduction in microbial load was assessed by plating the withdrawn samples onto nutrient agar plates and counting the colony-forming units after overnight incubation at 37 °C. Control experiments were also conducted without UV exposure to determine the baseline microbial concentration.

2.7. Groundwater characteristics

Upon arrival at the laboratory, groundwater samples underwent comprehensive analysis to evaluate various parameters critical for assessing water quality. These analyses involved employing specific methods, reagents, and test kits tailored to each category of compounds and elements present in the samples.

2.7.1. Organic compounds

Groundwater samples were analyzed for the presence of organic compounds, including HCG pesticides (α, β, γ-isomers) and DDT metabolites. Gas chromatography with electron capture detection (GC-ECD) was utilized as the primary method for detecting these compounds. Certified pesticide standards and high-purity solvents such as hexane and acetone were employed as reagents. The analysis was facilitated by using a Restek Rtx-CLPesticides column for efficient separation and detection of the target compounds.

2.7.2. Heavy metals

The analysis also encompassed the determination of heavy metal concentrations in the groundwater samples, including barium, cadmium, lead, arsenic, and others. Inductively coupled plasma mass spectrometry (ICP-MS) served as the preferred method for quantifying these metals due to its sensitivity and accuracy. Calibration standards and nitric acid of trace metal grade were utilized as reagents. The PerkinElmer NexION 2000 ICP-MS system was employed as the test kit for the analysis.

2.7.3. General mineral content and inorganic compounds

Furthermore, the groundwater samples were assessed for their general mineral content and inorganic compounds, such as calcium, chlorides, fluorides, nitrates, and nitrites. Ion chromatography (IC) was employed as the primary analytical technique for determining the concentrations of these ions. Standard solutions specific to each ion were used as reagents. The Dionex ICS-5000+ system served as the test kit for conducting the ion chromatography analysis.

2.7.4. Other parameters

Additional parameters, including cyanides, polyphosphates, total hardness (calcium and magnesium), silicic acid, and others, were also analyzed using specific methods and reagents tailored to each parameter. UV–visible spectrophotometry, titration methods, gravimetric analysis, and atomic absorption spectroscopy were among the techniques employed for these analyses.

2.7.5. Quality assurance and quality control (Q_A/Q_C)

Throughout the analysis process, stringent quality assurance and

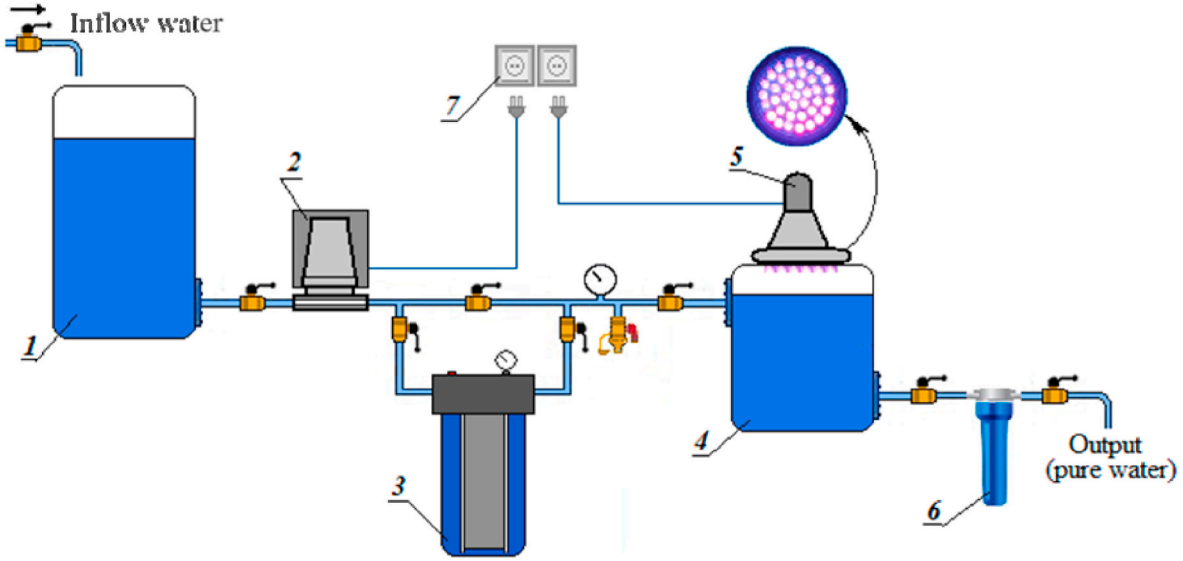

Fig. 1. Experimental setup; 1 - Initial water tank; 2 - Pump; 3 - Zeolite filter; 4 - UV treatment tank; 5 – UV lamp; 6 - Fine filter (membrane); 7 - Power supply.

quality control (Q_A/Q_C) measures were implemented to ensure the accuracy and reliability of the results. Daily calibration of instruments using certified standards, analysis of field blanks and duplicate samples to check for contamination and precision, inclusion of known concentration control samples to verify analytical accuracy, and cross-checking of results with historical data were among the Q_A/Q_C measures employed. These measures were vital in maintaining the integrity of the analytical process and ensuring the validity of the groundwater quality data obtained.

Table 2 presents various groundwater quality characteristics, including minimum (Min), maximum (Max), mean, median, and standard deviation (SD) values for each parameter. Parameters such as pH, turbidity, and concentrations of various ions and contaminants like calcium, chlorides, nitrates, and metals such as iron, manganese, and zinc are recorded. These values provide a comprehensive overview of the range and variability of groundwater quality parameters in the study area, offering valuable insights for understanding the baseline conditions and potential risks associated with groundwater use and management.

Table 2
Groundwater quality characteristics.

Parameter	Min	Max	Mean	Median	SD
Organic compounds					
HCG pesticides (α, β, γ-isomers) DDT and its metabolites	0.001	0.004	0.002	0.002	0.001
Phenol	0.001	0.002	0.002	0.002	0.0005
Oils	0.002	0.006	0.004	0.005	0.002
Heavy Metals					
Barium	0.1	0.3	0.167	0.1	0.094
Cadmium	0.001	0.002	0.001	0.001	0.0005
Lead	0.02	0.04	0.027	0.02	0.009
Arsenic	0.01	0.03	0.02	0.02	0.008
Beryllium	0.00002	0.00005	0.00004	0.00005	1.41×10^{-5}
Chromium	0.03	0.06	0.047	0.05	0.012
Copper	0.12	0.22	0.173	0.18	0.041
Hydrargyrum (Mercury)	0.0002	0.0004	0.0003	0.0002	9.43×10^{-5}
Manganese	34.8	56.5	45.6	45.5	8.859
Molybdenum	0.004	0.009	0.007	0.008	0.002
Nickel	0.01	0.01	0.01	0.01	0
Selenium	0.002	0.006	0.004	0.004	0.002
Zinc	0.01	0.02	0.013	0.01	0.005
General mineral content and inorganic compounds					
Calcium	48.65	80.32	63.03	60.12	13.092
Chlorides	144	195	170	171	20.833
Cyanides	0.022	0.046	0.034	0.035	0.01
Fluorides	0.2	0.3	0.23	0.2	0.047
Nitrates	0.32	0.56	0.453	0.48	0.1
Nitrites	0.001	0.006	0.003	0.003	0.002
Polyphosphates	0.022	0.044	0.03	0.028	0.009
Sulfates	138.43	189.98	165.09	166.85	21.082
Strontium	0.96	1.84	1.473	1.62	0.374
Total hardness	16.6	20.4	18.63	18.9	1.563
Aluminum	0.02	0.03	0.023	0.02	0.005
Boron	0.03	0.07	0.05	0.05	0.016
Iron	0.02	0.05	0.037	0.04	0.012
Silicic acid	10.8	13.6	12.43	12.9	1.19
Other physical and chemical parameters					
APAV	0.02	0.04	0.03	0.03	0.008
Colors	4.8	8.5	6.47	6.1	1.533
Dry residue	786.44	989.68	867.48	826.32	87.929
General mineralization	1465	1896	1691.667	1714	176.662
Permanganate oxidability	1.6	4.3	2.77	2.4	1.132
pH	7.85	8.45	8.18	8.24	0.249
Turbidity	0	2	1	1	0.816

2.8. Analytical methods

The concentrations of contaminants in groundwater samples were quantified using high-performance liquid chromatography (HPLC) for organic compounds, atomic absorption spectroscopy (AAS) for heavy metals, and turbidity measurements for suspended solids. The microbial load was enumerated by plating serial dilutions of groundwater samples on selective agar media followed by colony counting after incubation.

2.9. Statistical methods

Statistical analysis was conducted to assess the significance of experimental results and determine the optimal operating conditions for groundwater purification. Regression analysis was performed to correlate adsorption/desorption kinetics with process variables such as initial contaminant concentration, pH, temperature, and contact time. Additionally, goodness-of-fit tests were conducted to validate the applicability of adsorption isotherm and kinetic models to the experimental data. The adsorption capacity of zeolite for selected contaminants was evaluated by fitting experimental data to various adsorption isotherm models such as Langmuir and Freundlich equations. Kinetic studies were performed to assess the rate of adsorption and determine the kinetic parameters using pseudo-first-order and pseudo-second-order models.

2.9.1. Adsorption isotherm models

2.9.1.1. Langmuir isotherm. The Langmuir isotherm assumes monolayer adsorption onto a surface with a finite number of identical sites. It is described by the equation (Equation (1)) [35]:

$$q = \frac{Q_{max} \times K_L \times C}{1 + K_L \times C} \quad (1)$$

Whereby; q is the amount of adsorbate adsorbed per unit mass of adsorbent (adsorption capacity, usually in mg/g), C is the equilibrium concentration of adsorbate in solution (usually in mg/L), Q_{max} is the maximum adsorption capacity of the adsorbent (mg/g), K_L is the Langmuir adsorption constant (L/mg), representing the energy of adsorption.

2.9.1.2. Freundlich isotherm. The Freundlich isotherm assumes multilayer adsorption onto a heterogeneous surface. It is described by the equation (Equation (2)) [36]:

$$q = K_F \times C^{\frac{1}{n}} \quad (2)$$

Whereby; q is the amount of adsorbate adsorbed per unit mass of adsorbent (adsorption capacity, usually in mg/g), C is the equilibrium concentration of adsorbate in solution (usually in mg/L), K_F is the Freundlich constant related to adsorption capacity (mg/g) $(L/mg)^{1/n}$, n is the Freundlich exponent or heterogeneity factor (dimensionless).

2.9.2. Kinetic models

2.9.2.1. Pseudo-first-order kinetic model. The pseudo-first-order kinetic model assumes that the rate of adsorption is directly proportional to the number of unoccupied sites on the adsorbent surface. It is described by the equation (Equation (3)) [37]:

$$\log(q_e - q_t) = log\, q_e - \frac{K_1 \times t}{2.303} \quad (3)$$

Whereby; q_e is the amount of adsorbate adsorbed at equilibrium (mg/g), q_t is the amount of adsorbate adsorbed at time t (mg/g), k_1 is the rate constant of pseudo-first-order adsorption (1/min).

2.9.2.2. Pseudo-second-order kinetic model. The pseudo-second-order

kinetic model assumes that the rate of adsorption is controlled by chemisorption involving valency forces. It is described by the equation (Equation (4)) [38]:

$$\frac{t}{q_t} = \frac{1}{k_2 \times q_c^2} - \frac{1}{q_c} \times t \quad (4)$$

Whereby; q_e is the amount of adsorbate adsorbed at equilibrium (mg/g), q_t is the amount of adsorbate adsorbed at time t (mg/g), k_2 is the rate constant of pseudo-second-order adsorption (g/mg·min).

2.10. Cost analysis and scalibity potential

In this study, both cost analysis and scalability strategies were integrated to evaluate the economic feasibility and potential for widespread adoption of the proposed purification method. The cost analysis encompassed the expenses associated with acquiring materials like the calcination-modified zeolite and UV disinfection system, as well as the operational costs involved in implementing and maintaining the purification system over time. Alongside this, scalability considerations were incorporated to assess how the technology could adapt and perform across different scales of operation. Factors such as equipment costs, installation expenses, energy consumption, maintenance requirements, and labor costs were evaluated in light of potential scalability challenges.

3. Results

3.1. BET analysis

The results of the Brunauer-Emmett-Teller (BET) analysis revealed significant improvements in the physicochemical properties of the natural zeolite following the modification process (Table 3). The surface area increased from 60 m^2/g in the raw natural zeolite to 220 m^2/g in the modified zeolite, indicating a substantial enhancement in the available surface area for adsorption. Correspondingly, the pore volume also experienced a notable increase, rising from 0.15 cm^3/g to 0.8 cm^3/g, suggesting a greater capacity for adsorbate uptake. The average pore diameter expanded from 25 Å to 35 Å, indicating the presence of larger pores in the modified zeolite structure. Additionally, the modified zeolite exhibited a lower bulk density of 0.9 g/cm^3 compared to 1.2 g/cm^3 for the raw natural zeolite, suggesting a more porous and lightweight material. The higher crystallinity percentage of 95 % in the modified zeolite compared to 80 % in the raw material signifies an improved degree of structural order and stability. Furthermore, the particle size distribution narrowed from 5-50 μm to 2–20 μm, indicating a more uniform and refined particle size distribution in the modified zeolite.

3.2. Removal efficiency

The comparison of removal efficiency between natural and modified zeolite reveals a notable enhancement in the latter across various parameters (Fig. 2). The modified zeolite exhibits significantly higher removal efficiencies for most contaminants, indicating its superior performance in water treatment applications. Notably, the removal efficiencies for contaminants such as zinc, cadmium, and manganese show remarkable improvements with the modified zeolite, with removal efficiencies increasing from 30.25 % to 67.5 %, 55.75 %–82.75 %, and 64.04 %–69.52 %, respectively. Additionally, the modified zeolite demonstrates enhanced removal efficiencies for organic contaminants like phenol and cyanides, with efficiencies rising from 59.99 % to 73.26 % and 59.22 %–65.05 %, respectively. Moreover, parameters such as total hardness, nitrates, and general mineralization also show considerable improvements in removal efficiencies with the modified zeolite, indicating its effectiveness in addressing a wide range of water contaminants.

Table 3
Summary of the BET analysis results.

Property	Raw Natural Zeolite	Modified Zeolite
Surface Area (m^2/g)	60	220
Pore Volume (cm^3/g)	0.15	0.8
Average Pore Diameter (Å)	25	35
Bulk Density (g/cm^3)	1.2	0.9
Crystallinity (%)	80	95
Particle Size Distribution (μm)	5–50	2–20

3.3. Isotherms

The results from Freundlich and Langmuir isotherm models provide insights into the adsorption behavior of both natural and modified zeolite (Table 4). In the Freundlich model, the slope (k_f) represents the adsorption capacity of the material, indicating slightly higher values for natural zeolite (0.88) compared to modified zeolite (0.85), suggesting a relatively higher affinity of the natural zeolite for adsorbate molecules. The determination coefficient (R^2) reflects the goodness of fit of the model to the experimental data, with both natural and modified zeolites showing high R^2 values, indicating excellent fits. The intercept parameter (1/n) represents the adsorption intensity, with the modified zeolite exhibiting a higher value (1.1) compared to natural zeolite (0.78), implying a stronger adsorption intensity for the modified zeolite. Moving to the Langmuir model, the slope (q_{max}) represents the maximum adsorption capacity, with the natural zeolite showing a higher value (250 mg/g) compared to the modified zeolite (180 mg/g), indicating a higher adsorption capacity for the natural zeolite. Both materials exhibit high determination coefficients (R^2), suggesting good fits to the Langmuir model. The intercept (K_L) reflects the equilibrium constant, with slightly higher values observed for the modified zeolite (0.006) compared to natural zeolite (0.004), indicating a greater tendency for adsorption at lower concentrations for the modified zeolite. Additionally, the Rl parameter, indicating the favorability of adsorption, is higher for the modified zeolite (0.075) compared to natural zeolite (0.025), suggesting a higher favorability of adsorption for the modified zeolite.

3.4. Kinetics

The results from the kinetic modeling of adsorption processes using first and second-order kinetics reveal essential insights into the adsorption behavior of both natural and modified zeolite materials (Table 5). In the first-order kinetic model, the slope (k_L) represents the rate constant, with slightly lower values observed for the modified zeolite (−0.04642) compared to natural zeolite (−0.04831), indicating a slightly slower adsorption rate for the modified zeolite. Both materials exhibit moderate determination coefficients (R^2), suggesting a reasonable fit to the first-order model. The intercept parameter reflects the initial adsorption capacity, with the modified zeolite showing a slightly higher value (−0.66487) compared to natural zeolite (−0.5802), suggesting a higher initial adsorption capacity for the modified zeolite. Moving to the second-order kinetic model, both natural and modified zeolites exhibit high determination coefficients ($R^2 = 1$), indicating an excellent fit to the second-order model. The slope (k_2) represents the rate constant of the second-order adsorption process, with slightly lower values observed for the modified zeolite (0.03188) compared to natural zeolite (0.03381), indicating a slightly slower adsorption rate for the modified zeolite. The intercept parameter represents the initial adsorption capacity, with both natural and modified zeolites showing relatively low values (0.00253 and 0.00192, respectively), suggesting comparable initial adsorption capacities for both materials. Additionally, the equilibrium adsorption capacities (q_e) for both first and second-order kinetics are slightly higher for the modified zeolite (0.5143 mg/g and 31.37 mg/g, respectively) compared to natural zeolite (0.5598 mg/

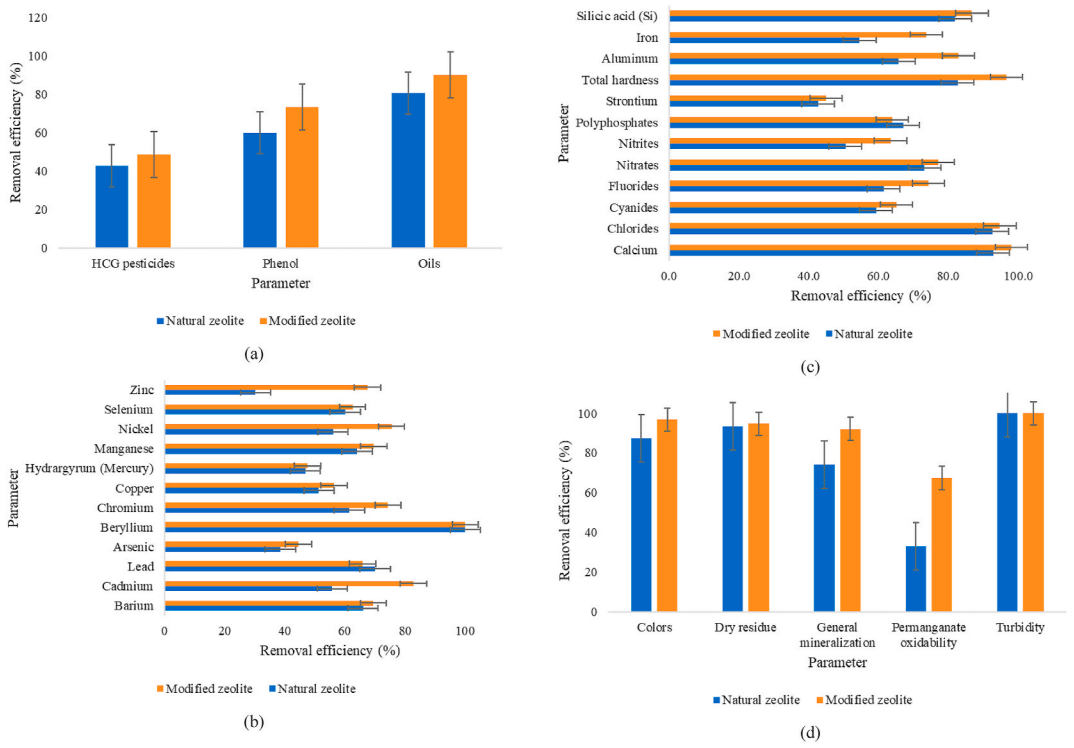

Fig. 2. Summary of the removal efficiency results for natural and modified zeolite (a) organic compounds (b) heavy metals (c) general mineral content and inorganic compounds (d) other physical and chemical properties.

Table 4
Summary of adsorption isotherm analysis.

Isotherm Model	Parameter	Natural Zeolite	Modified Zeolite
Freundlich	Slope (k_f)	0.88	0.85
	R^2	0.992	0.998
	Intercept (1/n)	0.78	1.1
	1/n	0.88	0.85
Langmuir	Slope (q_{max})	0.2	0.08
	R^2	0.999	0.999
	Intercept (K_L)	0.004	0.006
	q_{max} (mg/g)	250	180
	R_L	0.025	0.075

Table 5
Summary of adsorption kinetics analysis.

Kinetic Model	Parameter	Natural Zeolite	Modified Zeolite
First Order	Slope (k_L)	−0.04831	−0.04642
	R^2	0.67479	0.67315
	Intercept	−0.5802	−0.66487
	q_e (mg/g)	0.5598	0.5143
	q_e^2	–	–
Second Order	Slope (k_2)	0.03381	0.03188
	R^2	1	1
	Intercept	0.00253	0.00192
	q_e (mg/g)	29.58	31.37
	q_e^2	874.8	983.93

g and 29.58 mg/g, respectively), indicating a marginally improved adsorption capacity for the modified zeolite.

3.5. UV microbial elimination

The results illustrate the efficacy of natural and modified zeolite filtration coupled with UV disinfection in reducing microbial contamination levels in raw groundwater (Table 6). Raw groundwater typically contains high microbial counts, as evidenced by the initial counts of total coliforms (2245 CFU/mL), E. coli (543 CFU/mL), Enterococci (1089 CFU/mL), Pseudomonas aeruginosa (386 CFU/mL), and total heterotrophic bacteria (5141 CFU/mL). However, after filtration with natural zeolite and UV disinfection, there's a substantial reduction in microbial counts, with total coliforms decreasing to 8 CFU/mL, E. coli to 1 CFU/mL, Enterococci to 4 CFU/mL, Pseudomonas aeruginosa to 2 CFU/mL, and total heterotrophic bacteria to 18 CFU/mL. Further improvement is observed with modified zeolite filtration coupled with UV disinfection, where microbial counts are even lower, with total coliforms reduced to 3 CFU/mL, E. coli to 0 CFU/mL, Enterococci to 1 CFU/mL, Pseudomonas aeruginosa to 0 CFU/mL, and total heterotrophic bacteria to 8 CFU/mL.

Table 6
Microbial analysis results.

Microorganism	Raw Groundwater (CFU/mL)	Natural Zeolite Filtration + UV (CFU/mL)	Modified Zeolite Filtration + UV (CFU/mL)
Total Coliforms	2245	8	3
E. coli	543	1	0
Enterococci	1089	4	1
Pseudomonas aeruginosa	386	2	0
Total Heterotrophic	5141	18	8

3.6. Removal efficiency comparative analysis

Table 7 presents a comparative analysis of different treatment methods for contaminant removal from groundwater, along with their respective removal efficiencies as reported in various studies. The results demonstrate a wide range of removal efficiencies across the different methods. Notably, the calcination-modified zeolite, investigated in this study, exhibits the highest removal efficiency of up to 100 %. Other

Table 7
Summary of the removal efficiency comparative analysis.

Treatment Method	Removal Efficiency (%)	Reference
Calcination-modified zeolite	Up to 100	This study
Iron oxide-coated sand column filter	99	Callegari et al. [39]
Nanoscale zerovalent iron (Fe°)	89.7	Maamoun et al. [40]
Bimetallic nanoscale zerovalent iron (Fe°/Cu)	84.1	Maamoun et al. [40]
Activated carbon	23.01	Maamoun et al. [40]
Sand/zeolite mixture	14	Maamoun et al. [40]
Hydrothermally treated aluminosilicate clay	53	Obijole et al. [41]
Porous calcium alginate/graphene oxide composite aerogel	95.4 (lead), 81.2 (copper), 73.2 (cadmium)	Pan et al. [42]
Silver nanoparticles coated filters	100 (E. coli, S. typhimurium, S. dysenteriae, V. cholerae), 8–67 (other pathogens)	Mpenyana-Monyatsi et al. [43]
Moringa oleifera seeds	65-81 (lead)	Aziz et al. [44]
Musa cavendish peel	65-81 (lead)	Aziz et al. [44]
Sulfur-based mixotrophic bio-reduction	95.5	Zhang et al. [45]
Biological As(III) oxidation in biofilters	90	Crognale et al. [46]
Straw zerovalent iron and zerovalent iron-free sustainable-release carbon-compound material (ZVI-free SCCM)	>60	Wen et al. [47]

methods such as the iron oxide-coated sand column filter, nanoscale zerovalent iron (Fe°), and bimetallic nanoscale zerovalent iron (Fe°/Cu) also show high removal efficiencies ranging from 84.1 % to 99 %. Conversely, activated carbon and sand/zeolite mixture display relatively lower removal efficiencies of 23.01 % and 14 %, respectively. Additionally, alternative methods like hydrothermally treated aluminosilicate clay, porous calcium alginate/graphene oxide composite aerogel, and biological As(III) oxidation in biofilters demonstrate moderate to high removal efficiencies ranging from 53 % to 90 %. Interestingly, silver nanoparticles coated filters and plant-based materials such as Moringa oleifera seeds and Musa cavendish peel show variable removal efficiencies for different contaminants. Overall, the results highlight the effectiveness of various treatment methods for groundwater contaminant removal, providing valuable insights for water remediation efforts.

3.7. Cost analyisis anad scalability potential

Table 8 summarizes the cost analysis and scalability potential of implementing the proposed purification method using calcination-modified zeolite and UV disinfection. In terms of material costs, each unit of calcination-modified zeolite is estimated at $320, while each UV disinfection system unit costs $1520, resulting in a total material cost of $1840. Operational costs include installation expenses totaling $850 and annual maintenance costs of $520. Energy consumption per unit of water treated is estimated at 105 kWh, with a potential energy savings of 17 %. Routine maintenance is required bi-monthly, with additional maintenance tasks scheduled quarterly. Labor costs include installation labor at $32 per hour and routine maintenance labor at $27 per hour, resulting in total annual labor costs of $3150. The scalability potential section highlights the identification of potential scalability challenges and the analysis of strategies to mitigate these challenges, ensuring the efficient and effective scaling-up of the purification method as needed.

Table 8
Summary of the cost analysis and scalability potential.

Aspect	Findings
Material Costs	Calcination-modified zeolite: $320/unit UV disinfection system: $1520/unit Total material costs: $1840
Operational Costs	Installation expenses: $850 Annual maintenance costs: $520
Energy Consumption	Energy consumption: 105 kWh/unit Potential energy savings: 17 %
Maintenance Requirements	Routine maintenance: Bi-monthly Additional maintenance: Quarterly
Labor Costs	Installation labor: $32/hour Routine maintenance labor: $27/hour Total annual labor costs: $3150
Scalability Potential	Identification of potential scalability challenges Analysis of strategies to mitigate challenges

4. Discussion

The significant improvements observed in the physicochemical properties of the modified zeolite following the modification process can be attributed to several underlying mechanisms. Firstly, the increase in surface area from 60 m^2/g to 220 m^2/g suggests that the modification process effectively opened up more surface sites on the zeolite particles, enhancing the material's adsorption capacity. This increase in surface area is likely due to the removal of impurities and the restructuring of the zeolite lattice during the modification process, leading to a more porous structure with a higher number of active sites available for adsorption [23]. Correspondingly, the rise in pore volume from 0.15 cm^3/g to 0.8 cm^3/g indicates a greater capacity for adsorbate uptake within the modified zeolite structure, as there are more spaces available for molecules to be adsorbed. The increase in average pore diameter from 25 Å to 35 Å suggests the presence of larger pores in the modified zeolite, which can accommodate larger molecules and enhance the material's versatility in adsorption applications. Additionally, the lower bulk density of the modified zeolite (0.9 g/cm^3) compared to the raw natural zeolite (1.2 g/cm^3) indicates a more porous and lightweight material, which is desirable for filtration and adsorption processes. The higher crystallinity percentage of 95 % in the modified zeolite compared to 80 % in the raw material suggests an improved degree of structural order and stability, which can contribute to enhanced adsorption performance and durability. Furthermore, the narrowed particle size distribution from 5-50 μm to 2–20 μm indicates a more uniform and refined particle size distribution in the modified zeolite, which can lead to better packing and increased efficiency in adsorption processes. Overall, these improvements in physicochemical properties highlight the effectiveness of the modification process in enhancing the adsorption capacity and performance of natural zeolite for various environmental and industrial applications [48].

The removal efficiency results for various parameters using natural and modified zeolites demonstrate substantial improvements across several contaminants, with the modified zeolite consistently showing higher percentages. This enhanced performance can be attributed to the tailored modification process, which optimizes the zeolite's surface properties and adsorption capabilities. For instance, parameters like total hardness, phenol, nickel, oils, beryllium, aluminum, iron, lead, barium, cadmium, chlorides, calcium, dry residue, general mineralization, turbidity, and colors exhibit significant enhancement in removal efficiency with the modified zeolite, reaching typical values ranging from 65 % to 100 %. This improvement is attributed to the increased surface area and surface reactivity of the modified zeolite, enabling better adsorption and removal of these contaminants from the water. Furthermore, the removal mechanism involves the adsorption of contaminants onto the modified zeolite surface, where interactions such as ion exchange, electrostatic attraction, and chemical bonding occur. This mechanism enhances the removal efficiency by effectively capturing a wide range of contaminants present in the water. While some parameters like cyanides, manganese, nitrates, selenium, chromium, nitrites,

polyphosphates, fluorides, and silicic acid display moderate improvements, achieving typical values between 50 % and 80 %, the modified zeolite still demonstrates notable efficacy in their removal. The removal process for these contaminants involves similar mechanisms as mentioned earlier, albeit with varying degrees of affinity and selectivity towards the modified zeolite. On the other hand, contaminants such as arsenic, zinc, copper, and permanganate oxidability exhibit more varied results, typically ranging from 30 % to 70 % efficiency. The removal efficiency for these contaminants is influenced by factors such as their chemical speciation, concentration levels, and competing ions present in the water matrix. Despite the variability, the modified zeolite still demonstrates considerable potential in removing these contaminants, albeit with slightly lower efficiency compared to other contaminants. The findings obtained from this research align with those reported in existing literature. For example, in Onyutha et al.'s [49], investigation, the removal efficiencies for lead using natural zeolite within 20 and 40 minutes were 75 % and 98 %, respectively. Additionally, the elimination of As(III) with modified zeolite achieved a 91 % removal rate within a 10-min timeframe. Similarly, the removal of fluoride using modified zeolite yielded an 80 % efficiency within just 5 minutes.

The results from the Freundlich and Langmuir isotherm models shed light on the adsorption behavior of both natural and modified zeolite, revealing important insights into their respective capabilities. In the Freundlich model, the slightly higher slope (k_f) observed for natural zeolite compared to modified zeolite suggests a relatively higher adsorption capacity for the former, indicating a stronger affinity of natural zeolite for adsorbate molecules [36]. This difference could be attributed to the presence of certain functional groups or surface characteristics in the natural zeolite that promote stronger interactions with adsorbate species. Both natural and modified zeolites exhibit high determination coefficients (R^2), indicating excellent fits to the Freundlich model, which corroborates the validity of the adsorption behavior observed. The higher intercept parameter (1/n) for the modified zeolite suggests a stronger adsorption intensity compared to natural zeolite, implying that the modified zeolite has a greater tendency to adsorb molecules at lower concentrations, potentially due to modifications in its surface chemistry or pore structure [50]. Moving to the Langmuir model, despite the differences, both natural and modified zeolites exhibit high determination coefficients (R^2), indicating good fits to the Langmuir model and further confirming their adsorption behavior. Similarly, the slightly higher intercept parameter (K_L) for the modified zeolite implies a greater tendency for adsorption at lower concentrations, possibly due to alterations in the zeolite's surface properties or pore structure. Additionally, the higher R_L parameter for the modified zeolite suggests a higher favorability of adsorption compared to natural zeolite, indicating that the modified zeolite may have a more favorable adsorption environment or higher affinity for adsorbate species [51].

The results from the kinetic modeling of adsorption processes using first and second-order kinetics provide crucial insights into the adsorption behavior of both natural and modified zeolite materials. Both materials exhibit moderate determination coefficients (R^2), indicating a reasonable fit to the first-order model and confirming the applicability of this model to describe their adsorption behavior. Moreover, the slightly higher initial adsorption capacity observed for the modified zeolite, as indicated by the intercept parameter, suggests that the modification process may have enhanced the initial adsorption capacity of the material [52]. Moving to the second-order kinetic model, both natural and modified zeolites show excellent fits to the model, with high determination coefficients ($R^2 = 1$), indicating a perfect match between the experimental data and the model predictions. The slightly lower rate constant (k_2) observed for the modified zeolite suggests a slightly slower adsorption rate compared to natural zeolite, which may be attributed to changes in the zeolite's surface characteristics or pore structure resulting from the modification process. Despite this, both materials exhibit comparable initial adsorption capacities, as indicated by the intercept parameter. Additionally, the equilibrium adsorption capacities (q_e) for both first and second-order kinetics are slightly higher for the modified zeolite compared to natural zeolite, indicating a marginally improved adsorption capacity for the modified material.

The remarkable efficacy of natural and modified zeolite filtration combined with UV disinfection in reducing microbial contamination levels in raw groundwater can be attributed to several underlying mechanisms. Initially, raw groundwater contains high microbial counts due to the presence of various microorganisms, including bacteria like total coliforms, E. *coli, Enterococci*, and *Pseudomonas aeruginosa*. When subjected to filtration with zeolite, the porous structure of the material facilitates the physical adsorption of microorganisms, effectively trapping them within its matrix. Zeolite's inherent antimicrobial properties, attributed to its surface chemistry and ion exchange capabilities, also contribute to microbial removal by disrupting cell membranes and inhibiting microbial growth [53]. The subsequent UV disinfection process further enhances microbial inactivation by exposing the trapped microorganisms to UV radiation, which damages their DNA and prevents replication [54]. This combined approach ensures thorough microbial reduction, as evidenced by the substantial decrease in microbial counts post-filtration and UV treatment [55]. Moreover, the modification of zeolite may enhance its adsorption capacity and antimicrobial activity, resulting in even lower microbial counts after treatment. Overall, the synergistic action of zeolite filtration and UV disinfection offers a robust and effective solution for microbial control in groundwater, safeguarding public health and ensuring the provision of safe drinking water.

The breakdown of material costs revealed a substantial investment required for both the modified zeolite and UV disinfection systems, contributing to a total material cost of $1840. Operational costs, including installation expenses and annual maintenance, further added to the overall expenses. However, the potential energy savings of 17 % offered a promising avenue for reducing long-term operational costs. Additionally, the labor costs associated with installation and routine maintenance underlined the importance of considering human resource expenditures in the implementation phase. The identified routine maintenance requirements, along with the scheduled additional maintenance tasks, highlighted the ongoing commitment necessary for the upkeep of the purification system. Furthermore, the discussion of scalability potential underscored the need for proactive measures to address potential challenges that might have arisen with the scaling-up of the purification method, ensuring its efficient and sustainable deployment to meet varying demands for safe drinking water. Overall, these findings provided a comprehensive overview of the economic considerations and scalability prospects associated with the proposed water purification approach, aiding in informed decision-making and strategic planning for its implementation. In the study conducted by Sorg et al. [56], on the expenses incurred by small drinking water systems in arsenic removal from groundwater, the authors detailed the capital and operation and maintenance (O&M) costs of 48 treatment systems, varying in capacity from 10 to 770 gallons per minute (gpm) (equivalent to 38–2915 L per minute). The capital costs of these systems spanned from $477 to $6171 per gpm ($126–$1632 per L/min) of design flow, while the O&M costs ranged from $0.07 to $22.88 per 1000 gallons ($0.02–$6.05 per 1000 L) of treated water.

5. Conclusion

This study investigated the efficacy of modified zeolite filtration coupled with UV disinfection as a comprehensive solution for mitigating microbial contamination in raw groundwater. The conclusions drawn from this study underscored the significant advancements achieved in water purification technology through the application of modified zeolite filtration combined with UV disinfection. Our findings highlighted the superior adsorption performance of modified zeolite compared to its natural counterpart, as evidenced by enhancements in physicochemical properties such as increased surface area, pore volume,

and crystallinity. Isotherm and kinetic modeling further elucidated the improved adsorption capacity and kinetics of modified zeolite, emphasizing its enhanced efficiency in removing contaminants. Particularly noteworthy were the substantial improvements observed in the removal efficiencies of various contaminants, including zinc, cadmium, manganese, phenol, and cyanides. Moreover, parameters like total hardness, nitrates, and general mineralization also exhibited significant enhancements in removal efficiencies with modified zeolite, indicating its efficacy across a diverse range of water contaminants. Notably, achieving up to 100 % removal efficiency for turbidity and beryllium underscored the robust performance of the modified zeolite filtration system. Furthermore, our experimental results demonstrated a remarkable reduction in microbial contamination levels in raw groundwater post-treatment, highlighting the efficacy of the combined approach in delivering safe drinking water. These findings pave the way for the widespread implementation of modified zeolite filtration and UV disinfection in water treatment facilities and community-level purification systems, thereby ensuring access to clean and potable water and promoting sustainable development on a global scale. Moving forward, the integration of modified zeolite filtration and UV disinfection holds immense promise for widespread implementation in water treatment facilities and community-level purification systems. By leveraging these innovative technologies, we can ensure access to clean and potable water, thereby safeguarding human health and promoting sustainable development worldwide.

Funding

This research was funded by the Science Committee of the Ministry of Science and Higher Education of the Republic of Kazakhstan (Grant No. AP14972646), Development of green technology of groundwater treatment for drinking purposes using natural zeolites of Kazakhstan, for the years 2022–2024.

CRediT authorship contribution statement

Kulyash Meiramkulova: Supervision, Resources, Project administration, Methodology, Investigation, Conceptualization. **Aliya Kydyrbekova:** Methodology, Investigation, Funding acquisition, Formal analysis, Conceptualization. **Timoth Mkilima:** Writing – review & editing, Writing – original draft, Methodology, Investigation, Conceptualization. **Tursynkul Bazarbayeva:** Resources, Investigation. **Umbetova Sholpan:** Resources, Investigation. **Mansur Zarbaliyev:** Resources, Investigation. **Tatyana Uryumtseva:** Resources, Investigation. **Laura Kurbanova:** Resources, Investigation. **Bayan Tussupova:** Resources, Investigation. **Mikhail Zhumagulov:** Resources, Investigation.

Declaration of competing interest

The authors declare that they have no known competing financial interests or personal relationships that could have appeared to influence the work reported in this paper.

Data availability

Data will be made available on request.

References

[1] T. Mkilima, Groundwater salinity and irrigation suitability in low-lying coastal areas. A case of Dar es Salaam, Tanzania, Watershed Ecol. Environ. 5 (2023) 173–185, https://doi.org/10.1016/j.wsee.2023.07.002.
[2] S. Kurwadkar, Occurrence and distribution of organic and inorganic pollutants in groundwater, Water Environ. Res. (2019), https://doi.org/10.1002/wer.1166.
[3] K.G. Coronado-Apodaca, S.E. Rodríguez-De Luna, R.G. Araújo, M.A. Oyervides-Muñoz, G.M. González-Meza, L. Parra-Arroyo, J.E. Sosa-Hernandez, H.M.N. Iqbal, R. Parra-Saldivar, Occurrence, transport, and detection techniques of emerging pollutants in groundwater, MethodsX 10 (2023) 102160, https://doi.org/10.1016/j.mex.2023.102160.
[4] A.L. Srivastav, Chemical fertilizers and pesticides: role in groundwater contamination, in: Agrochem. Detect. Treat. Remediat., Elsevier, 2020, pp. 143–159, https://doi.org/10.1016/B978-0-08-103017-2.00006-4.
[5] Z. Xiang, S. Wu, L. Zhu, K. Yang, D. Lin, Pollution characteristics and source apportionment of heavy metal(loid)s in soil and groundwater of a retired industrial park, J. Environ. Sci. 143 (2024) 23–34, https://doi.org/10.1016/j.jes.2023.07.015.
[6] F. Rehman, T. Cheema, Effects of sewage waste disposal on the groundwater quality and agricultural potential of a floodplain near Jeddah, Saudi Arabia, Arabian J. Geosci. 9 (2016) 307, https://doi.org/10.1007/s12517-016-2340-y.
[7] S. Hube, M. Eskafi, K.F. Hrafnkelsdóttir, B. Bjarnadóttir, M.Á. Bjarnadóttir, S. Axelsdóttir, B. Wu, Direct membrane filtration for wastewater treatment and resource recovery: a review, Sci. Total Environ. 710 (2020) 136375, https://doi.org/10.1016/j.scitotenv.2019.136375.
[8] Y. Feng, L. Yang, J. Liu, B.E. Logan, Electrochemical technologies for wastewater treatment and resource reclamation, Environ. Sci. Water Res. Technol. 2 (2016) 800–831, https://doi.org/10.1039/C5EW00289C.
[9] M. Pritchard, T. Mkandawire, A. Edmondson, J.G. O'Neill, G. Kululanga, Potential of using plant extracts for purification of shallow well water in Malawi, Phys. Chem. Earth (2009), https://doi.org/10.1016/j.pce.2009.07.001.
[10] X. Yang, G. Huang, C. An, X. Chen, J. Shen, J. Yin, P. Song, Z. Xu, Y. Li, Removal of arsenic from water through ceramic filter modified by nano-CeO2: a cost-effective approach for remote areas, Sci. Total Environ. 750 (2021) 141510, https://doi.org/10.1016/j.scitotenv.2020.141510.
[11] K. Meiramkulova, D. Orynbekov, G. Saspugayeva, K. Aubakirova, S. Arystanova, A. Kydyrbekova, E. Tashenov, K. Nurlan, T. Mkilima, The effect of mixing ratios on the performance of an integrated poultry slaughterhouse wastewater treatment plant for a recyclable high-quality effluent, Sustain. Times (2020), https://doi.org/10.3390/su12156097.
[12] D. Marghade, G. Mehta, S. Shelare, G. Jadhav, K.C. Nikam, Arsenic contamination in Indian groundwater: from origin to mitigation approaches for a sustainable future, Water (Switzerland) (2023), https://doi.org/10.3390/w15234125.
[13] M.H.C. Harun, M.I. Ahmad, A. Jusoh, A. Ali, S. Hamzah, Rapid-Slow sand filtration for groundwater treatment: effect of filtration velocity and initial head loss, Int. J. Integr. Eng. (2022), https://doi.org/10.30880/ijie.2022.14.01.026.
[14] S. Amiri, V. Vatanpour, T. He, Optimization of coagulation-flocculation process in efficient arsenic removal from highly contaminated groundwater by response surface methodology, Molecules (2022), https://doi.org/10.3390/molecules27227953.
[15] G. Temesgen, A. Lelago, E. Assefa, A. Admasie, Evaluation of chlorination efficiency on improving microbiological and physicochemical parameters in water samples available in Sheble Berenta district Amhara region, Ethiopia, Appl. Water Sci. 13 (2023) 120, https://doi.org/10.1007/s13201-023-01922-5.
[16] L. Velarde, M.S. Nabavi, E. Escalera, M.-L. Antti, F. Akhtar, Adsorption of heavy metals on natural zeolites: a review, Chemosphere 328 (2023) 138508, https://doi.org/10.1016/j.chemosphere.2023.138508.
[17] K. Meiramkulova, A. Kydyrbekova, D. Devrishov, U. Nurbala, A. Tuyakbayeva, S. Zhangazin, R. Ualiyeva, V. Kolpakova, Y. Yeremeyeva, T. Mkilima, Comparative analysis of natural and synthetic zeolite filter performance in the purification of groundwater, Water (Switzerland) (2023), https://doi.org/10.3390/w15030588.
[18] T. Mkilima, D. Devrishov, K. Assel, N. Ubaidulayeva, A. Tleukulov, A. Khassenova, N. Yussupova, D. Birimzhanova, Natural zeolite for the purification of saline groundwater and irrigation potential analysis, Molecules 27 (2022) 7729, https://doi.org/10.3390/molecules27227729.
[19] M. Mohaghegh Montazeri, F. Taghipour, Virtual prototyping and characterization of a point-of-entry UV-LED water disinfection reactor with the synergic effect of radiation, hydrodynamics, and inactivation kinetics, Water Res. 230 (2023) 119581, https://doi.org/10.1016/j.watres.2023.119581.
[20] O. Abdelwahab, W.M. Thabet, Natural zeolites and zeolite composites for heavy metal removal from contaminated water and their applications in aquaculture Systems: a review, Egypt, J. Aquat. Res. (2023), https://doi.org/10.1016/j.ejar.2023.11.004.
[21] V. Krstić, Role of zeolite adsorbent in water treatment, in: Handb. Nanomater. Wastewater Treat., Elsevier, 2021, pp. 417–481, https://doi.org/10.1016/B978-0-12-821496-1.00024-6.
[22] S. Chałupnik, W. Franus, M. Wysocka, G. Gzyl, Application of zeolites for radium removal from mine water, Environ. Sci. Pollut. Res. (2013), https://doi.org/10.1007/s11356-013-1877-5.
[23] E. Kuldeyev, M. Seitzhanova, S. Tanirbergenova, K. Tazhu, E. Doszhanov, Z. Mansurov, S. Azat, R. Nurlybaev, R. Berndtsson, Modifying natural zeolites to improve heavy metal adsorption, Water (Switzerland) (2023), https://doi.org/10.3390/w15122215.
[24] D. Wu, Y. Sun, L. Wang, Z. Zhang, J. Gui, A. Ding, Modification of NaY zeolite by lanthanum and hexadecyl trimethyl ammonium bromide and its removal performance for nitrate, Water Environ. Res. 92 (2020) 987–996, https://doi.org/10.1002/wer.1285.
[25] O. Cadar, Z. Dinca, M. Senila, A. Becze, F. Todor, Studies on the modification of some natural zeolite from nw Romania after acid and basic treatments, Int. Multidiscip. Sci. GeoConference Surv. Geol. Min. Ecol. Manag. SGEM (2020), https://doi.org/10.5593/sgem2020/1.1/s01.039.
[26] S. Boycheva, S. Miteva, I. Trendafilova, D. Zgureva, M. Václavíková, M. Popova, Magnetite nanoparticles activated coal fly ash zeolites with application in waste

water remediation, in: Proc. 16th Int. Conf. Environ. Sci. Technol., 2022, https://doi.org/10.30955/gnc2019.00560.
[27] S. Li, G. Huang, X. Kong, Y. Yang, F. Liu, G. Hou, H. Chen, Ammonium removal from groundwater using a zeolite permeable reactive barrier: a pilot-scale demonstration, Water Sci. Technol. 70 (2014) 1540–1547, https://doi.org/10.2166/wst.2014.411.
[28] A.M. Siemens, J.J. Dynes, W. Chang, Sodium adsorption by reusable zeolite adsorbents: integrated adsorption cycles for salinised groundwater treatment, Environ. Technol. 42 (2021) 3083–3094, https://doi.org/10.1080/09593330.2020.1721567.
[29] B. Kwakye-Awuah, B. Sefa-Ntiri, E. Von-Kiti, I. Nkrumah, C. Williams, Adsorptive removal of iron and manganese from groundwater samples in Ghana by zeolite y synthesized from bauxite and kaolin, Water (Switzerland) (2019), https://doi.org/10.3390/w11091912.
[30] E. Yogafanny, K.O. Yohan, A. Sungkowo, Treatment of brackish groundwater by zeolite filtration in sumur tua wonocolo, kedewan, bojonegoro, east java, IOP Conf. Ser. Earth Environ. Sci. 212 (2018) 012014, https://doi.org/10.1088/1755-1315/212/1/012014.
[31] N.M. Hull, W.H. Herold, K.G. Linden, UV LED water disinfection: validation and small system demonstration study, AWWA Water Sci (2019), https://doi.org/10.1002/aws2.1148.
[32] P.O. Nyangaresi, T. Rathnayake, S.E. Beck, Evaluation of disinfection efficacy of single UV-C, and UV-A followed by UV-C LED irradiation on Escherichia coli, B. spizizenii and MS2 bacteriophage, in water, Sci. Total Environ. (2023), https://doi.org/10.1016/j.scitotenv.2022.160256.
[33] X.Y. Zou, Y.L. Lin, B. Xu, T.C. Cao, Y.L. Tang, Y. Pan, Z.C. Gao, N.Y. Gao, Enhanced inactivation of E. coli by pulsed UV-LED irradiation during water disinfection, Sci. Total Environ. (2019), https://doi.org/10.1016/j.scitotenv.2018.08.367.
[34] N.S. Salikova, J. Rodrigo-Ilarri, K.K. Alimova, M.-E. Rodrigo-Clavero, Analysis of the water quality of the Ishim River within the Akmola region (Kazakhstan) using hydrochemical indicators, Water 13 (2021) 1243, https://doi.org/10.3390/w13091243.
[35] D.A. Castro, D.H. Pereira, P.V.B. Leal, Langmuir isotherm: kinetic and equilibrium considerations, Periódico Tchê Química 16 (2019) 324–334, https://doi.org/10.52571/PTQ.v16.n31.2019.330_Periodico31_pgs_324_334.pdf.
[36] M. Vigdorowitsch, A. Pchelintsev, L. Tsygankova, E. Tanygina, Freundlich isotherm: an adsorption model complete framework, Appl. Sci. 11 (2021) 8078, https://doi.org/10.3390/app11178078.
[37] H. Moussout, H. Ahlafi, M. Aazza, H. Maghat, Critical of linear and nonlinear equations of pseudo-first order and pseudo-second order kinetic models, Karbala Int. J. Mod. Sci. (2018), https://doi.org/10.1016/j.kijoms.2018.04.001.
[38] Y. Miyake, H. Ishida, S. Tanaka, S.D. Kolev, Theoretical analysis of the pseudo-second order kinetic model of adsorption. Application to the adsorption of Ag(I) to mesoporous silica microspheres functionalized with thiol groups, Chem. Eng. J. 218 (2013) 350–357, https://doi.org/10.1016/j.cej.2012.11.089.
[39] A. Callegari, N. Ferronato, E.C. Rada, A.G. Capodaglio, V. Torretta, Assessment of arsenic removal efficiency by an iron oxide-coated sand filter process, Environ. Sci. Pollut. Res. (2018), https://doi.org/10.1007/s11356-018-2674-y.
[40] I. Maamoun, O. Eljamal, O. Falyouna, R. Eljamal, Y. Sugihara, Multi-objective optimization of permeable reactive barrier design for Cr(VI) removal from groundwater, Ecotoxicol. Environ. Saf. (2020), https://doi.org/10.1016/j.ecoenv.2020.110773.
[41] O. Obijole, G.W. Mugera, R. Mudzielwana, P. Ndungu, A. Samie, A. Babatunde, Hydrothermally treated aluminosilicate clay (HTAC) for remediation of fluoride and pathogens from water: adsorbent characterization and adsorption modelling, Water Resour. Ind. 25 (2021) 100144, https://doi.org/10.1016/j.wri.2021.100144.
[42] P.L. Yap, M.J. Nine, K. Hassan, T.T. Tung, D.N.H. Tran, D. Losic, Graphene-based sorbents for multipollutants removal in water: a review of recent progress, Adv. Funct. Mater. (2021), https://doi.org/10.1002/adfm.202007356.
[43] L. Mpenyana-Monyatsi, N.H. Mthombeni, M.S. Onyango, M.N.B. Momba, Cost-effective filter materials coated with silver nanoparticles for the removal of pathogenic bacteria in groundwater, Int. J. Environ. Res. Publ. Health 9 (2012) 244–271, https://doi.org/10.3390/ijerph9010244.
[44] N.A.A. Aziz, N. Jayasuriya, L. Fan, A. Al-Gheethi, A low-cost treatment system for underground water using <scp> *Moringa oleifera* </scp> seeds and *Musa cavendish* peels for remote communities, J. Chem. Technol. Biotechnol. 96 (2021) 680–696, https://doi.org/10.1002/jctb.6581.
[45] Y. Zhang, F. Jin, Z. Shen, F. Wang, R. Lynch, A. Al-Tabbaa, Adsorption of methyl tert-butyl ether (MTBE) onto ZSM-5 zeolite: fixed-bed column tests, breakthrough curve modelling and regeneration, Chemosphere 220 (2019) 422–431, https://doi.org/10.1016/j.chemosphere.2018.12.170.
[46] S. Crognale, B. Casentini, S. Amalfitano, S. Fazi, M. Petruccioli, S. Rossetti, Biological As(III) oxidation in biofilters by using native groundwater microorganisms, Sci. Total Environ. 651 (2019) 93–102, https://doi.org/10.1016/j.scitotenv.2018.09.176.
[47] W. Zhang, N. Shan, Y. Bai, L. Yin, The innovative application of agriculture straw in in situ field permeable reactive barrier for remediating nitrate-contaminated groundwater in grain-production areas, Biochem. Eng. J. 164 (2020) 107755, https://doi.org/10.1016/j.bej.2020.107755.
[48] M. Senila, O. Cadar, Modification of natural zeolites and their applications for heavy metal removal from polluted environments: challenges, recent advances, and perspectives, Heliyon 10 (2024) e25303, https://doi.org/10.1016/j.heliyon.2024.e25303.
[49] C. Onyutha, E. Okello, R. Atukwase, P. Nduhukiire, M. Ecodu, J.N. Kwiringira, Improving household water treatment: using zeolite to remove lead, fluoride and arsenic following optimized turbidity reduction in slow sand filtration, Sustain. Environ. Res. 34 (2024) 4, https://doi.org/10.1186/s42834-024-00209-x.
[50] N. Halalsheh, O. Alshboul, A. Shehadeh, R.E. Al Mamlook, A. Al-Othman, M. Tawalbeh, A. Saeed Almuflih, C. Papelis, Breakthrough curves prediction of selenite adsorption on chemically modified zeolite using boosted decision tree algorithms for water treatment applications, Water (Switzerland) (2022), https://doi.org/10.3390/w14162519.
[51] M. Popaliya, A. Mishra, Modified zeolite as an adsorbent for dyes, drugs, and heavy metal removal: a review, Int. J. Environ. Sci. Technol. (2023), https://doi.org/10.1007/s13762-022-04603-z.
[52] J.-P. Simonin, On the comparison of pseudo-first order and pseudo-second order rate laws in the modeling of adsorption kinetics, Chem. Eng. J. 300 (2016) 254–263, https://doi.org/10.1016/j.cej.2016.04.079.
[53] Y.L. Li, D.T. McCarthy, A. Deletic, Stable copper-zeolite filter media for bacteria removal in stormwater, J. Hazard Mater. 273 (2014) 222–230, https://doi.org/10.1016/j.jhazmat.2014.03.036.
[54] M.S. Makuei, F. Ketabchi, N. Peleato, Impact of water characteristics on UV disinfection of unfiltered water, Water Qual. Res. J. (2022), https://doi.org/10.2166/wqrj.2022.006.
[55] K. Meiramkulova, A. Temirbekova, G. Saspugayeva, A. Kydyrbekova, D. Devrishov, Z. Tulegenova, K. Aubakirova, N. Kovalchuk, A. Meirbekov, T. Mkilima, Performance of a combined treatment approach on the elimination of microbes from poultry slaughterhouse wastewater, Sustain. Times (2021), https://doi.org/10.3390/su13063467.
[56] T.J. Sorg, L. Wang, A.S.C. Chen, The costs of small drinking water systems removing arsenic from groundwater, J. Water Supply Res. Technol. 64 (2015) 219–234, https://doi.org/10.2166/aqua.2014.044.